CONTROL OF FILM UNIFORMITY PROPERTIES IN A PLANETARY RADIAL-FLOW GALLIUM NITRIDE CVD SYSTEM

Rinku P. Parikh * **Raymond A. Adomaitis** *

* *Department of Chemical Engineering and Institute for Systems Research University of Maryland, College Park MD 20742*

Abstract: The development and application of a geometrically-based uniformity criterion is presented for film uniformity optimization in a radial-flow GaN epitaxy reactor system. In this multi-wafer reactor system, individual wafers rotate on a rotating susceptor in a planetary motion to reduce the effects of reactant depletion on deposition uniformity; the uniformity criterion developed for this system gives an unambiguous criterion for minimizing non-uniformity of any film property, can be implemented in a run-to-run uniformity control scheme, and gives physical insight into the reactor operating conditions that most influence uniformity. Copyright 2005 IFAC.

Keywords: Chemical Vapor Deposition, Uniformity Control, Distributed Parameter Systems, Simulation

1. INTRODUCTION

Gallium nitride (GaN) is a compound semiconductor material that has shown tremendous potential in electronic and optoelectronic devices over the past few years due to its wide-bandgap and high breakdown field properties. GaN has a direct bandgap of 3.4 eV making it suitable for manufacturing light emitting diodes (LEDs) capable of emitting light of any wavelength between blue and ultraviolet (UV) when alloyed with indium (In) and aluminum (Al). In addition, GaN-based devices are used for high-frequency and/or high-power applications including aircraft radar electronics (Burk *et al.*, 1999).

Metalorganic vapor phase epitaxy (MOVPE) is the principal method used to grow single crystalline layers of this material. Gas phase gallium nitride chemistry can be visualized as consisting of competing reaction routes which can be broadly split between adduct formation and thermal decomposition pathways (Fig. 1). Each pathway is responsible for producing an array of chemical species that may eventually participate in GaN deposition. The primary gas phase reaction is the spontaneous interaction between commonly used precursors, trimethylgallium ($(CH_3)_3Ga$) and ammonia (NH_3), to form stable Lewis acid-Lewis base adducts (Almond *et al.*, 1992) and (Mazzarese *et al.*, 1989). Adduct formation is a ubiquitous problem during MOVPE of GaN and has been widely studied. Upon formation, these adducts may condense on cold surfaces inside the reactor system (Kisker and Kuech, 1993). For this reason, the formation of these adducts is believed to degrade film quality, uniformity, and consume the feed stream of organometallic sources (Zaouk *et al.*, 1981). NH_3 also undergoes minimal thermal decomposition at typical MOVPE conditions. A review of GaN

Fig. 1. Gas phase reactions involving Ga-containing compounds.

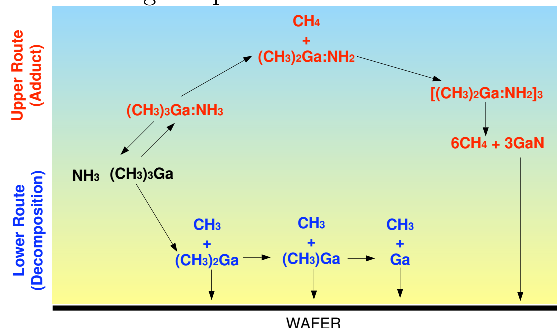

related gas-phase and surface reaction chemistry is given in (Parikh and Adomaitis, 2004).

Consequently, numerous research groups have designed reactor systems, in particular gas delivery systems, with the intent to minimize precursor interactions. The most common approach is to use separate injectors to reduce any premature mixing of the precursors (Theodoropoulos *et al.*, 2001) and (Safvi *et al.*, 1997); radial flow geometry reactors are designed to compensate for reactant depletion by incorporating a planetary wafer rotation system, where a ring of wafers arranged on a large rotating susceptor rotate themselves.

Recently, an approach to film uniformity control in planetary reactor systems was proposed in (Adomaitis, 2004) based purely on the geometry of radial flow reactors with this mode of wafer rotation. In this approach, a sequence of stalled-wafer (non-rotating) deposition profiles are identified that, when rotated, produce perfectly uniform films. Then, a deposition profile, produced either by simulation or by an actual CVD process is projected onto this sequence of uniformity-producing profiles to compute the "Nearest Uniformity Producing Profile" (NUPP), which under rotation would produce a uniform film. Thus, it becomes clear that one would want to drive the current profile to the "nearest" profile, NUPP, giving an unambiguous optimization criterion. Most importantly, the NUPP provides the process engineer with physical insight on how reactor operating conditions should be modified to drive the current profile towards the NUPP to improve uniformity. This technique is extremely powerful because it can be applied to not only film thickness but any distributed film quality for either process development or in a run-to-run control system.

2. UNIFORMITY CONTROL CRITERION

A vertical cross-sectional view of a radial-flow planetary reactor system along with its physical domain, $R_0 \leq R \leq R_{sus}$, is shown in Figure 2. The precursors and carrier gas species are injected into the center of the reactor through a 2-flow

Fig. 2. A cross-sectional view of radial-flow planetary reactor with a 2-flow gas inlet design (top); and the physical domain (bottom).

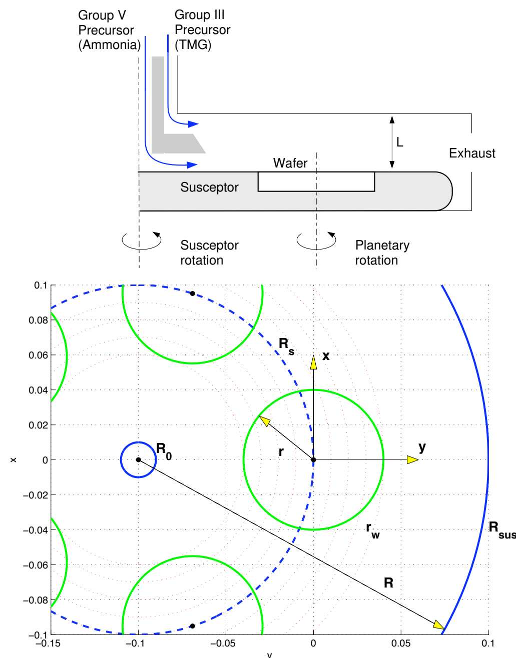

gas inlet design and flow outwards over wafers arranged in a circular pattern over the susceptor. The 2-flow gas inlet design allows group III compounds to be introduced separately from group V compounds. In these reactors, the wafers are placed on rotating satellites which in turn rotate around the central axis of the susceptor plate. The radial flow geometry combined with the substrate planetary motion mechanism is commonly employed to produce uniform deposition profiles on the wafers (Frijlink, 1988). It should be noted that reactors of this type can be run with both rotating and stalled (non-rotating) wafers.

2.1 Uniformity modes

Using the notation of (Adomaitis, 2004), we summarize the derivation of the uniformity producing modes and the uniformity optimization criterion. For this analysis, $\Delta(R)$ is defined as the 1-dimensional deposition profile over the susceptor radial coordinate and Ω is the interval of R corresponding to the location of the wafer; $\omega : \ 0 \leq r \leq r_w$ is the wafer radial coordinate. If $\delta(r, \theta)$ is the 2-dimensional profile that results when $\Delta(R)$ is projected onto the stalled (non-rotating) wafer physical domain, wafer rotation will eliminate the θ dependence by averaging the film quality over θ giving

$$\bar{\delta}(r) = \frac{1}{2\pi} \int_0^{2\pi} \Delta \left(\sqrt{r^2 \cos^2 \theta + (r \sin \theta + R_s)^2} \right) d\theta.$$

Any profile $\Delta(R)$ over the wafer segment domain $R \in \Omega$ can be represented by a shifted Legendre polynomial sequence expansion

$$\Delta(R) = \sum_{m=0}^{\infty} a_m P_m(R);$$

The expansion approximation results in

$$\bar{\delta}(r) = \sum_{m=0}^{\infty} \frac{a_m}{2\pi} \int_0^{2\pi} P_m \left(\sqrt{r^2 \cos^2\theta + (r\sin\theta + R_s)^2} \right) d\theta$$
$$= \sum_{m=0}^{\infty} a_m \alpha_m(r) \qquad \text{in } \omega.$$

The goal is to find non-uniform $\Delta(R)$ profiles that produce uniform $\bar{\delta}(r)$ profiles under rotation, a criterion that can be written in terms of the minimization problem

$$\min_{a_m} || \sum_{m=1}^{M} a_m \alpha_m(r) - c || \qquad (1)$$

where c is a constant with respect to r and can be set $c = 1$ in (1) without loss of generality. Note that $m = 0$ is not used in this criterion: $P_0 = 1$ and so must produce a uniform α_0.

Defining the array $\mathbf{Q}$ of inner products over ω,

$$Q_{i,j} = \int_0^{r_w} \alpha_j \alpha_i \, r dr \qquad i = 1, \cdots, M, \; j = 1, \cdots, M$$

$$\mathbf{Q} = \mathbf{U} \mathbf{\Sigma} \mathbf{V}^T \qquad (2)$$

where the singular value decomposition (SVD) (2) produces $\mathbf{U}^{M \times M}$ containing the (orthogonal) left singular vectors and $\mathbf{\Sigma}$ the singular values. From these products of the SVD, we define an orthogonal set of basis functions $\{\alpha_n^v\}_{n=1}^N$ using

$$\alpha_n^v = \sum_{m=1}^{M} U_{m,n} \alpha_m(r)$$

for the space spanned by the $\{\alpha_m\}_{m=1}^M$. Observing the singular values of $\mathbf{Q}$ used to define the α_n^v, the set of relatively small magnitude σ_m indicate there are fewer than M α_n^v necessary to span the space of the sequence $\{\alpha_m\}_{m=1}^M$.

These calculations lead to the definition of the first non-flat deposition mode that generates perfectly uniform films when rotated:

$$\beta_1(R) = \sum_{m=1}^{M} b_m P_m(R)$$

where $\beta_0 =$ constant and

Fig. 3. The first four β_n modes projected onto the stalled wafer.

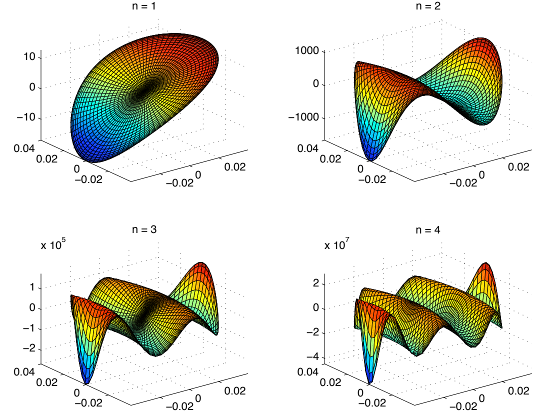

$$b_m = \sum_{n=1}^{N} U_{m,n} a_n^v$$

where the a_n^v are computed using (1) and the reduced basis $\{\alpha_m^v\}_{m=1}^N$.

The procedure described above produces a single β_n profile; sequentially removing the lower-frequency α_j^v from the problem of finding the a_j^v that minimizes ϵ_N (refer to (3)) will force the minimization procedure to find a progression of modes correspondingly increasing in frequency. Therefore, we can produce additional β_n modes by minimizing the sequence of problems

$$\epsilon_N = \min_{a_j^v} || \sum_{j=n}^{N} a_j^v \alpha_j^v - 1 || \qquad (3)$$

for $n = 2, 3, \ldots$ to obtain the corresponding β_n.

Projecting the β_n onto the stalled wafer domain, we observe illustrated in Figure 3 the first four non-flat deposition profiles that produce perfectly uniform profiles when rotated. Because these modes define at least part of a basis for the uniformity producing subspace of all possible deposition profiles, any linear combination of the β_n modes is guaranteed to produce a uniform deposition profile under rotation. These modes depend only on the wafer and susceptor geometry, therefore are truly universal in their nature.

2.2 Planetary Radial-Flow CVD Reactor Model Development

A one-dimensional model describing gas temperature and composition is developed for this reactor system. The equation of continuity for the total gas molar flow rate is used to obtain the gas velocity

$$\frac{d}{dR}(v\rho R) = 0 \qquad \textit{or} \qquad v = \frac{v_0 R_0 T}{T_0 R} \qquad (4)$$

where the assumption of the ideal gas law is used to determine an explicit relationship between temperature (T), radial position (R) and gas velocity (v); R_0 denotes the radius of the central feed tube and v_0 is the inlet gas velocity. The energy balance equation in cylindrical coordinates is obtained by assuming the heat capacity (C_p) and thermal conductivity (k) of the carrier gas are independent of temperature; the parameter values are evaluated using the average of the inlet temperature (T_{inlet}) and susceptor temperature (T_S):

$$\frac{C_p}{R}\frac{d}{dR}(R\rho vT) = \frac{k}{R}\frac{d}{dR}(R\frac{dT}{dR}) + \frac{2k}{L^2}(T_S - T) \quad (5)$$

with boundary conditions

$$T = T_{inlet} \,\text{at}\, R = R_0, \quad \frac{dT}{dR} = 0 \,\text{at}\, R = R_{sus} \quad (6)$$

Here, T_S represents the constant susceptor temperature and L is the spacing between the wafer top surface and the reactor roof which is assumed to be perfectly insulating. A material balance is written for each chemical species

$$\frac{1}{R}\frac{d}{dR}(cx_iv) = R_i^G + \frac{R_i^S}{L/2} \quad (7)$$

where c is the total concentration of the gas ($c = P/R_{gas}/T$ for an ideal gas, P is the total reactor pressure, and R_{gas} corresponds to the ideal gas constant), x_i is the mole fraction of the ith species, R_i^G the rate of generation of species i per unit volume due to gas phase reactions and R_i^S the rate of generation of species i per unit area due to surface phase reactions; the model assumes that deposition occurs only on the susceptor surface. The quantity $L/2$ represents the distance that Ga-containing precursors must travel in order to adsorb onto the wafer surface after the gas leaves the divided region (refer to Figure 2). Inlet boundary conditions for each chemical species material balance equation are the known mole fractions at the inlet, $x_i(R = R_0) = x_{i0}$.

The modeling equations thus are defined by a coupled set of one- and two-point boundary-value problems. To obtain steady-state temperature and deposition rate profiles, the modeling equations are discretized on a Gaussian quadrature grid, and a Newton-Raphson technique is used to drive the residual corresponding to each discretized differential equation and boundary condition to zero. An object-oriented MATLAB-based weighted residual tool-box (Adomaitis, 2002) is used to carry out these computations. The same quadrature-based MWR tools are used to compute the β_n modes and to project deposition profiles onto these modes to compute the NUPP, described in the next section.

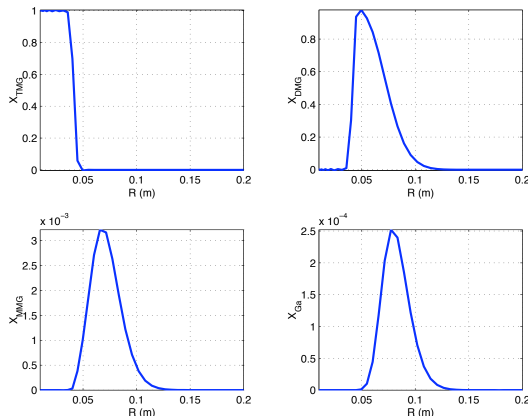

Fig. 4. Simulation results illustrating normalized chemical species profiles.

A representative set of operating parameters used to deposit gallium nitride for this reactor geometry is taken from (Beccard *et al.*, 1999). In their planetary reactor system, they reported the following operating conditions: pressure 37.5 torr, susceptor temperature (T_S) 1373 K, and a total flow 6.5 slm. Based on these parameters and assuming that the total flowrate of 6.5 slm is split equally between the top and bottom inlets, $T_{inlet} = 300K$ and $L = 1.5cm$ (Frijlink, 1988), an initial value for $v_0 = 3.85m/s$ is computed. $R_0 = 0.01m$, susceptor radius $R_{sus} = 0.2m$, satellite wafer centerline radius $R_s = 0.1m$ and wafer radius $r_w = 0.04m$. The sum of the fluxes of monomethylgallium (MMG) and elemental gallium (Ga) are assumed to govern the growth rate and, accordingly, their surface reaction chemistry is also included in the computation.

Simulation results describing mole fraction profiles of each chemical species for the representative operating conditions are shown in Figure 4. The composition profiles are normalized with respect to the inlet TMG mole fraction. It is evident from the results that TMG is rapidly consumed well before the wafer location and that the only species present over the wafer are DMG, MMG, and Ga. This is directly related to the rapid gas heating inside the reactor which encourages the dissociation of the first methyl group from TMG. Because no TMG is present over the wafer, the adduct pathway (upper route) is suppressed as NH_3 begins mixing with the organometallic stream shortly before the wafer location, illustrating how reactor geometry influences deposition kinetics.

2.3 Uniformity Optimization

The deposition rate profile is a function of the gas phase mole fraction of MMG and Ga and is given by

$$\Delta(R) = R_{MMG}^S \cdot x_{MMG} + R_{Ga}^S \cdot x_{Ga} \quad (8)$$

Fig. 5. Wafer deposition profile Δ, resulting profile upon rotation $\bar{\delta}$, and the NUPP f and its profile upon rotation $\bar{f}$.

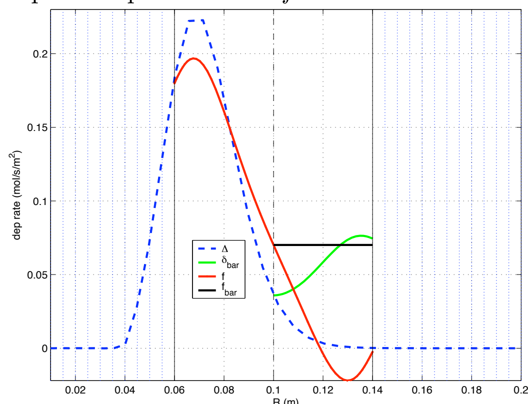

For the planetary reactor deposition system simulation under consideration, the "nearest" deposition rate profile f that generates a uniform film upon rotation is shown in Figure 5. This optimal profile f, henceforth referred to as the NUPP (Nearest Uniformity Producing Profile), is computed as the projection of the deposition profile $\Delta(R)$ onto the (normalized) β_n:

$$f = \sum_{n=1}^{N} \beta_n \int_{0}^{r_w} \Delta(R) \beta_n \, r dr$$

Defining C_d as the distance between f and Δ at the wafer center $R = R_s$ ($R_s = 0.1$ in this diagram), we are guaranteed of uniformity in the center region of the wafer when C_d vanishes. This gives an unambiguous design criterion of $C_d = 0$ for improved wafer uniformity in the central region of the wafer - in many cases, the region where uniformity is most desired.

In Figure 5, it is clear this criterion ($C_d = 0$) is not met, seeing as, δ_{bar}, the profile that results from rotation of the current $\Delta(R)$, is not uniform. However, the results immediately indicate that uniformity can be achieved in the wafer central region if current deposition rate profile were shifted upward and to the right to minimize C_d. Physical intuition based on knowledge of gallium nitride growth chemistry suggests decreasing the susceptor temperature as a potential means to improving uniformity relative to the original set of operating conditions.

A decrease in susceptor temperature will reduce the rates of the decomposition reactions, which in turn, will spread the peak of $\Delta(R)$ and push it toward the downstream direction. At the same time, lowering the susceptor temperature also will decrease the deposition rate. A minimization procedure was implemented to find the optimal susceptor temperature that minimizes C_d, guaranteeing a uniform deposition rate profile in the neighborhood of the wafer center. For this reactor system, we find the optimal susceptor temperature to be $T_S = 1312.60$ K. This analysis also reveals that the C_d value approaches zero at very low susceptor temperatures. This is expected because minimal decomposition of the precursor occurs in this regime causing $\Delta(R)$ to be nearly zero. Figure 6 clearly shows the improvement is uniformity in the center region of the wafer using the optimal susceptor temperature.

Fig. 6. Results for optimal susceptor temperature of $T_{sus} = 1312.60$ K (total flowrate=6.5 slm).

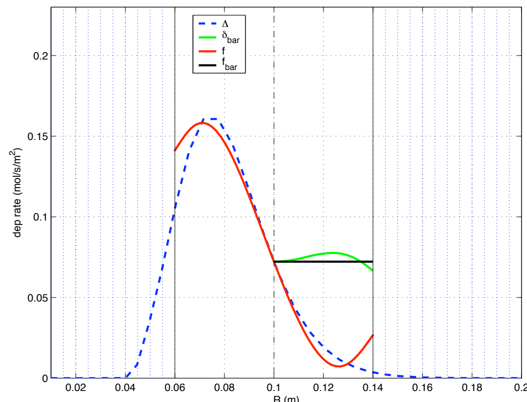

Fig. 7. Results for optimal susceptor temperature of $T_{sus} = 1200$ K (total flowrate=3.5 slm).

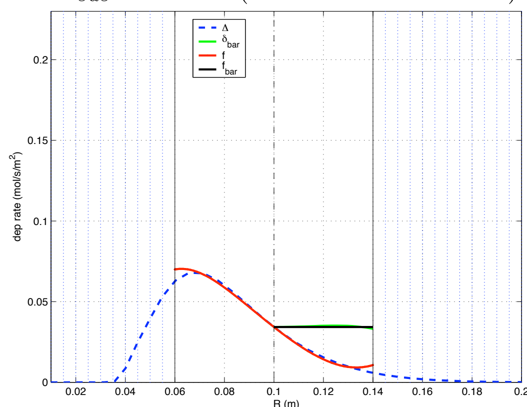

However, it is also obvious from Figure 6 that some degree of nonuniformity still exists towards the outer portion of the wafer. This occurs because $\Delta(R)$ and f do not completely overlap at the two ends of the wafer location. These results imply that modifying the susceptor temperature alone cannot be used to achieve uniform films over the entire wafer surface for this reactor system for a fixed set of other operating conditions. As a result, an analysis of the combined effect of susceptor temperature and total feed flowrate is performed. A measure of the nonuniformity is defined as

$$\chi = \sqrt{\int_{0}^{r_w} (\delta_{bar} - f_{bar})^2 \, r dr}. \tag{9}$$

The total flowrate is decreased from 6.5 slm to 3.5 slm by increments of 1 slm and the computation of C_d with respect to susceptor temperature is performed in each case to find the optimal values of the parameters. The results indicate that low flowrates lead to a reduction in nonuniformity. Under these conditions, the optimal susceptor temperature occurs at $T_S = 1200$ K and the results for the rotated profiles are shown in Figure 7. These results immediately convey the improvement in uniformity towards the outer portion of the wafer. The reason for this improvement is attributable to the lower total flowrate's effect of increasing reactor residence times, pushing the peak of the deposition rate profile ($\Delta(R)$) closer to the nearest uniformity producing profile (f).

2.4 Implementation of the Uniformity Control Criterion

The reactor system illustrated in Fig. 2 can process 5 wafers in a single deposition run; to implement a run-to-run control algorithm based on driving C_d to zero, the reactor system would be operated with 4 of the 5 production wafers undergoing rotating and a single sacrificial stalled wafer. After each deposition run, the stalled wafer deposition profile would be measured and projected onto the β_n modes to obtain the NUPP, C_d, and values for other criteria, such as χ. The reactor deposition model then would be used to determine a search direction based on minimizing the uniformity criteria, and the reactor operating conditions would be adjusted accordingly. Details of the implementation of this run-to-run control procedure as applied to an industrial CVD system will be described in a subsequent paper.

3. CONCLUDING REMARKS

A new approach to uniformity control was applied to a gallium nitride radial-flow chemical vapor deposition system with planetary wafer rotation. This approach provides a process engineer with physical insight on what design parameter(s) should be adjusted to improve uniformity. The results showed that by modifying the susceptor temperature, uniform films of gallium nitride can be produced upon rotation in the planetary radial-flow reactor system.

ACKNOWLEDGMENTS

The authors gratefully acknowledge the support and collaboration of Drs. Deborah P. Partlow, Michael E. Aumer, and Darren B. Thomson of the Northrop Grumman Corporation.

REFERENCES

Adomaitis, R.A. (2002). Objects for mwr. *Comp. & Chem. Engng.* **26**, 981–998.

Adomaitis, R.A. (2004). Identification of a deposition rate profile subspace corresponding to spatially-uniform films in planetary cvd reactors: A new criterion for uniformity control. *Comp. & Chem. Engng., in press.*

Almond, M.J., C.E. Jenkins, D.A. Rice and K. Hagen (1992). Organometallic precursors to the formation of gan by mocvd: structural characterisation of me3ganh3 by gas-phase electron diffraction. *J. Organomet. Chem.* **439**, 251–261.

Beccard, R., D. Schmitz, E.G. Woelk, G. Strauch, Y. Makarov, M. Heuken, M. Deschler and H. Juergensen (1999). High temperature cvd systems to grow gan or sic based structures. *J. Mat. Sci. and Eng.* **B61-62**, 314–319.

Burk, A.A. Jr., M.J. O'Loughlin, R.R. Siergiej, A.K. Agarwal, S. Sriram, R.C. Clarke, M.F. MacMillan, V. Balakrishna and C.D. Brandt (1999). Sic and gan wide bandgap semiconductor materials and devices. *Solid State Electronics* **43**, 1459–1464.

Frijlink, P.M. (1988). A new versatile, large size movpe reactor. *J. Crystal Growth* **93**, 207–215.

Kisker, D.W. and T.F. Kuech (1993). In: *The principles and practice of organometallic vapor phase epitaxy in: D.T.J. Hurle (Ed.), Handbook of Crystal Growth.* Vol. 3. Chap. 3. Elsevier Science. Amsterdam.

Mazzarese, D., A. Tripathi, W.C. Conner, K.A. Jones, L. Calderon and W. Eckart (1989). In situ ftir and surface analysis of the reaction of trimethylgallium and ammonia. *J. Electron. Mater.* **18**, 369–377.

Parikh, R.P. and R.A. Adomaitis (2004). An overview of gallium nitride growth chemistry and its effect on reactor design: Application to a radial-flow cvd system. *submitted for publication.*

Safvi, S.A., J.M. Redwing, M.A. Tischler and T.F. Kuech (1997). Gan growth by metallorganic vapor phase epitaxy: A comparison of modeling and experimental measurements. *J. Electrochem. Soc.* **144**, 1789–1796.

Theodoropoulos, C., T.J. Mountziaris, H.K. Moffat and J. Han (2001). Design of gas inlets for the growth of gallium nitride by metalorganic vapor phase epitaxy. *J. Cryst. Growth* **217**, 65–81.

Zaouk, A., E. Salvetat, J. Sakaya, F. Maury and G. Constant (1981). Various chemical mechanisms for the crystal growth of iii v semiconductors using coordination compounds as starting material in the mocvd process. *J. Cryst. Growth* **55**, 135–144.